PERGAMON
Available online at www.sciencedirect.com
SCIENCE DIRECT®
Polyhedron 22 (2003) 2133–2138
POLYHEDRON
www.elsevier.com/locate/poly

Host–guest chemistry of radical-copper wheels. A supramolecular control of magnetic exchange coupling

Takayuki Ishida *, Junichi Omata, Takashi Nogami

Department of Applied Physics and Chemistry, The University of Electro-Communications, Chofu, Tokyo 182-8585, Japan

Received 6 October 2002; accepted 11 January 2003

Abstract

The crystal of the hexanuclear wheel-shaped complex, $[\mathrm{CuCl_2 \cdot (4PMNN)}]_6$ (**1**), has a channel structure in a direction perpendicular to the molecular plane (4PMNN = 4-pyrimidinyl nitronyl nitroxide). Excess LiCl, NaCl, or KCl added to a methanol solution of **1** yielded the corresponding guest-included compounds, $(\mathrm{LiCl})_6$@**1**, $(\mathrm{NaCl})_2$@**1**, and $(\mathrm{KCl})_2$@**1**. The inclusion of the guests was confirmed by means of elemental analysis and X-ray diffraction study. The crystallographic *c* length and the cell volume were slightly shrunk by the guest inclusion. The ferromagnetic interaction, which is ascribed to intermolecular contacts between the nitronyl nitroxide groups, was remarkably enhanced almost in proportion to the cell shrinkage. Similar enhancement was observed for the host–guest complexes from the bromide analogue $[\mathrm{CuBr_2 \cdot (4PMNN)}]_6$. The crystallization in the presence of water gave $(\mathrm{H_2O})_n$@**1**. In addition to enhancement of the ferromagnetic interaction of $(\mathrm{H_2O})_n$@**1**, we found that the ferromagnetic interaction decreased back to a level of that of the empty **1** after removal of $\mathrm{H_2O}$ by evacuation.

Keywords: Ferromagnetic interaction; Supramolecule; Channel; Nitroxide; Ligand; Free radical

1. Introduction

Self-assembled discrete oligonuclear complexes with paramagnetic transition metal-ions have fascinated chemists owing to their architectural beauty as well as their mesoscopic physical properties [1]. Supramolecular techniques such as host–guest complex formation have been applied to fine-tune molecule-based magnetic materials [2]. In the course of our study on the role of radical-substituted pyrimidine (PM) as ferro- and antiferromagnetic couplers, we have found that discrete hexanuclear arrays $[\mathrm{CuX_2 \cdot (4PMNN)}]_6$ (**1**: X = Cl; **2**: X = Br; 4PMNN = 4-pyrimidinyl nitronyl nitroxide) exhibited ferromagnetic intermolecular interactions [3]. The crystals of **1** and **2** have a channel structure in a direction perpendicular to the molecular plane (Fig. 1) [3,4], and we named them 'magnetic nanotubes' [4] since the channel has a diameter of 11.5 Å defined with the opposing Cu···Cu distance. The crystal structure analysis of **1** and **2** suggests that the inner axial sites of the copper(II) ion are partially hydrated with the occupancy of the water molecule as small as 0.3 [3]. Host–guest complexation of these porous complexes was attempted because the vacant sites are assumed to be available for further coordination from guest molecules.

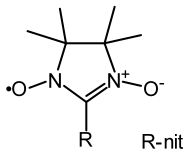

R-nitronyl nitroxide
(RNN)

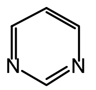

pyrimidine
(PM)

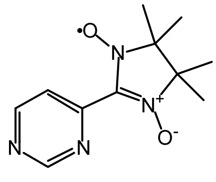

4PMNN

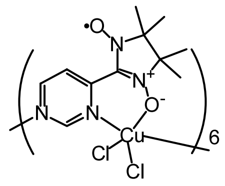

1

While conventional host compounds such as crown ethers possess lone-pairs inside as metal-ion binding

---

* Corresponding author. Tel.: +81-424-43-5490; fax: +81-424-43-5501.

E-mail address: ishi@pc.uec.ac.jp (T. Ishida).

0277-5387/03/$ - see front matter © 2003 Elsevier Science Ltd. All rights reserved.
doi:10.1016/S0277-5387(03)00206-7

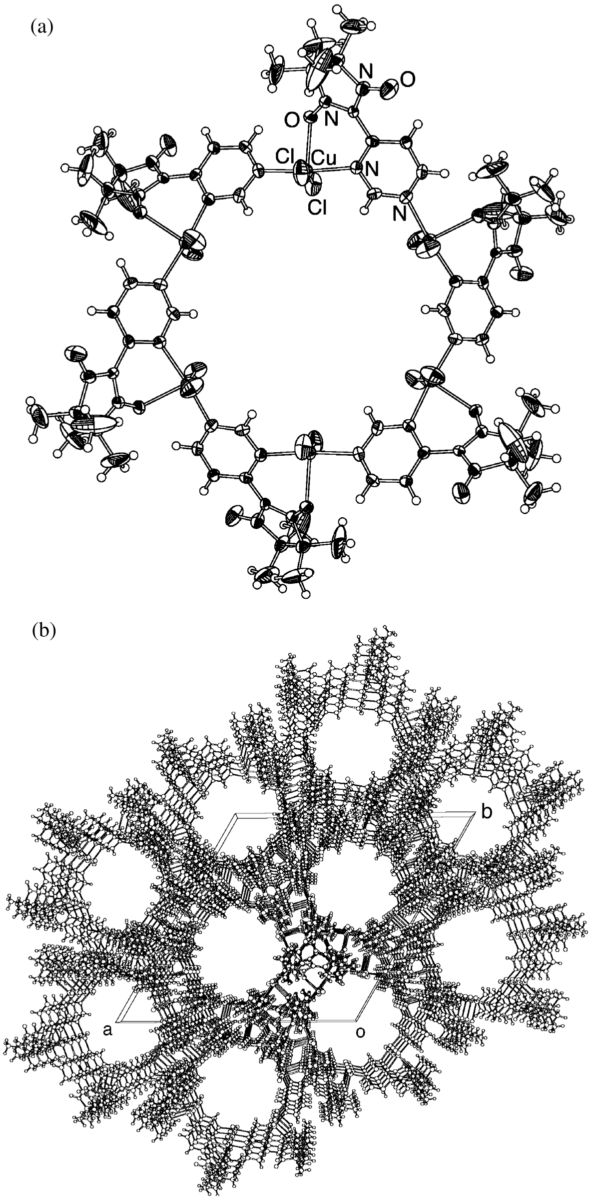

Fig. 1. (a) Molecular structure of **1**. (b) Molecular arrangement in the crystal of **1** viewed along the *c* axis.

sites, **1** and **2** conversely have lone-pair accepting sites inside. Thus, amines, acids, and halides are candidates for guest molecules in the present study. Actually, some organic molecules such as 1,3,5-tricarboxylbenzene were found to be incorporated in **1** [4]. We will report here new host–guest complexes of **1** with alkali-metal chlorides, namely, $(MCl)_n@\mathbf{1}$. Very interestingly, they showed remarkable enhancement of the ferromagnetic interaction compared with that of **1** itself. In addition to the enhancement, we also found that reduction of the ferromagnetic interaction in the hydrated complex, $(H_2O)_n@\mathbf{1}$, after removal of water by evacuation.

2. Experiments

Complex **1** as an almost empty specimen was synthesized according to the reported method [3]. Host–guest complexation was carried out by means of co-crystallization. The following procedure is typical. A homogenous methanol solution (12 ml) containing 4PMNN (42.1 mg, 0.18 mmol), $CuCl_2 \cdot 2H_2O$ (32.7 mg, 0.19 mmol), and a guest material LiCl (35.7 mg, 0.85 mmol) was allowed to stand at room temperature for 2 days. Black needles were precipitated from the above mixture and collected on a filter. In the case of hydration, to a clear methanol solution (8 ml) containing 4PMNN (33.0 mg, 0.14 mmol) and $CuCl_2 \cdot 2H_2O$ (23.1 mg, 0.14 mmol) was added water (0.5 ml), and black needles were precipitated and collected.

The dehydration experiment of $(H_2O)_n@\mathbf{1}$ was carried out as follows. After the magnetic susceptibility of freshly prepared $(H_2O)_n@\mathbf{1}$ was measured in a usual capsule-type holder, the capsule was picked up out of a magnetometer probe, opened carefully, and subjected to evacuation in a vacuum desiccator with an oil rotary pump for 2 days. The capsule was capped again and the magnetic properties of the sample in the same capsule were measured under the same conditions as the first measurement.

Elemental analyses (C, H, N) were done on a Fisons EA-1108 by a usual combustion method. X-Ray diffraction data were collected on a Raxis-Rapid IP diffractometer (Rigaku). The cell constants of the host–guest complexes were determined using graphite monochromated Cu Kα radiation at 298 ± 2 K. Magnetic susceptibilities of randomly oriented polycrystalline samples were measured on a Quantum Design MPMS SQUID magnetometer equipped with a 7 T coil in a temperature range 1.8–300 K. The magnetic responses were corrected with diamagnetic blank data of the sample holder obtained separately. The diamagnetic contribution of the sample itself was estimated from Pascal's constants.

3. Results

Co-crystallization methods afforded polycrystalline samples of $(MCl)_n@\mathbf{1}$, which apparently has the same

Table 1
Elemental analysis of $(MCl)_n@\mathbf{1}$ and **1**

	C	N	H (%)
$(LiCl)_6(4PMNN \cdot CuCl_2)_6$	31.50 (32.06)	13.41 (13.60)	2.27 (3.67)
$(NaCl)_2(4PMNN \cdot CuCl_2)_6$	33.69 (33.94)	13.72 (14.39)	4.77 (3.89)
$(KCl)_2(4PMNN \cdot CuCl_2)_6$	33.70 (33.48)	13.72 (14.20)	4.77 (3.83)
$(4PMNN \cdot CuCl_2)_6$	36.19 (35.74)	14.79 (15.15)	4.39 (4.09)

Calculated values are written in parenthesis.

crystal habit as that of the empty complex (**1**). Table 1 summarizes the results of elemental analysis on $(MCl)_n@\mathbf{1}$ and **1**. This analysis clearly demonstrates the presence of guest molecules in the co-crystallized specimens from comparison with that of **1**, and suggests the following formula, $(LiCl)_6@\mathbf{1}$, $(NaCl)_2@\mathbf{1}$, and $(KCl)_2@\mathbf{1}$. To clarify whether the guest molecules are located in an endohedral or exohedral position of the macrocyclic structure, X-ray crystallographic analysis was carried out on single crystals. The specimens belong to a rhombohedral crystal system with cell constants similar to those of **1**. Although the analysis of $(MCl)_n@\mathbf{1}$ revealed the presence of appreciable electron densities within a tube, especially in the inner axial site of the copper(II) ions, the atomic positions of the guest molecules could not be determined precisely owing to disorder. We can report only the cell constants of these complexes (Table 2). The cell constants were varied beyond the standard deviations as the guest molecules are incorporated but the cell dimensions were not so expanded as expected from the complex formation. These findings indicate that the molecular structure of the host (**1**) is retained and that the guest molecules are incorporated within a tube; thus, these complexes are expressed as $(\text{guest})_n@\mathbf{1}$. In the case of the hydrated complex the water molecules seems to escape readily [3] because the elemental analysis of $(H_2O)_n@\mathbf{1}$ showed poor reproducibility.

The magnetic properties of $(MCl)_n@\mathbf{1}$, $(H_2O)_n@\mathbf{1}$, and **1** were measured on a SQUID magnetometer under the same conditions. Fig. 2(a) summarizes the temperature dependences of the product of the molar magnetic susceptibility (χ_{mol}) and T for them. The peak formation of the $\chi_{mol}T$ value around 7 K for **1** is ascribed both to the *intermolecular ferromagnetic* and intramolecular antiferromagnetic interactions [3,4]. Upon cooling from 100 K, the $\chi_{mol}T$ values of the host–guest complexes of **1** increased more significantly and reached a higher maximum than that of **1** itself. The similarity of their magnetic behavior strongly indicates that the same magnetic coupling mechanism is involved and that structural perturbation from the original host (**1**) lead to the enhancement of the ferromagnetic coupling.

Fig. 2(b) shows the preliminary results on the bromide analogue. Complexation of 4PMNN and $CuBr_2$ gave the corresponding macrocyclic compound (**2**), and host–guest compounds are similarly prepared according to the co-crystallization method, affording $(MBr)_n@\mathbf{2}$ and $(H_2O)_n@\mathbf{2}$. The magnetic susceptibility measurements under the same conditions as those of the chloride analogues also showed enhancement of the ferromagnetic coupling.

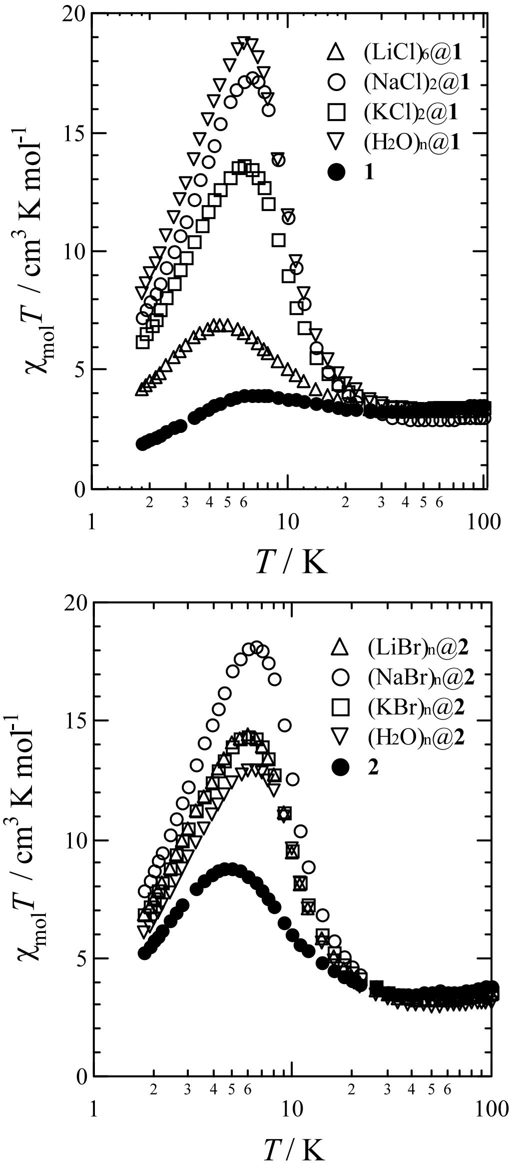

Fig. 2. Temperature dependence of the product of χ_{mol} and T measured at 5000 Oe for $(MCl)_n@\mathbf{1}$, $(H_2O)_n@\mathbf{1}$, and **1** (a) and $(MCl)_n@\mathbf{2}$, $(H_2O)_n@\mathbf{2}$, and **2** (b).

Table 2
Cell constants of $(MCl)_n@\mathbf{1}$, $(H_2O)_n@\mathbf{1}$, and **1**

	a (Å)	c (Å)	V (Å^3)
$(LiCl)_6@\mathbf{1}$	28.122(3)	12.415(3)	8502(2)
$(NaCl)_2@\mathbf{1}$	28.247(2)	12.254(2)	8467(2)
$(KCl)_2@\mathbf{1}$	28.1(1)	12.39(7)	8517(51)
1	28.261(2)	12.378(1)	8561(1)

$\alpha = \beta = 90°$, $\gamma = 120°$, $a = b$.

In order to exploit reversible control of magnetic couplings, we examined water molecules as a guest. Fig. 3 shows the temperature dependences of $\chi_{mol}T$ values for $(H_2O)_n@\mathbf{1}$ before and after evacuation. Before evacuation, with a decrease of temperature the $\chi_{mol}T$ value of $(H_2O)_n@\mathbf{1}$ increased more significantly than that of **1** itself just like $(MCl)_n@\mathbf{1}$. After evacuation, the $\chi_{mol}T$ value was almost coincident with that of **1**. The change is quite drastic as indicated with an arrow in Fig.

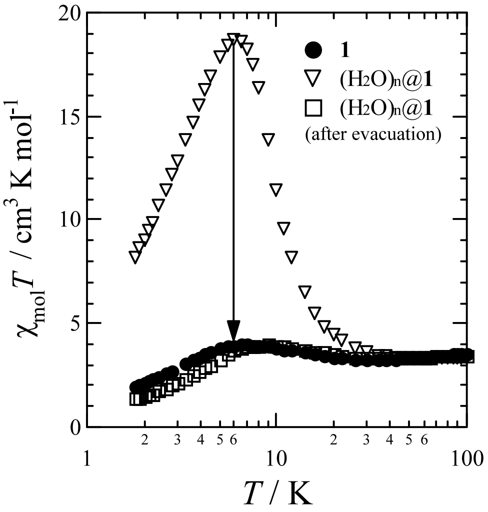

Fig. 3. Temperature dependence of the product of χ_{mol} and T of freshly prepared $(H_2O)_n@\mathbf{1}$ and evacuated $(H_2O)_n@\mathbf{1}$ together with that of **1** measured at 5000 Oe.

3. This finding supports that the molecular and crystal structures of the host (**1**) are preserved during the evacuation process and the enhancement of the ferromagnetic coupling is caused by the guest inclusion. We further attempted to repeat the enhancement of the magnetic coupling by moisture adsorption. After the specimen was allowed to stand in a humid atmosphere its magnetic susceptibility was measured under the same conditions. However, such an enhancement could not be observed probably because of failure of water adsorption.

4. Discussion

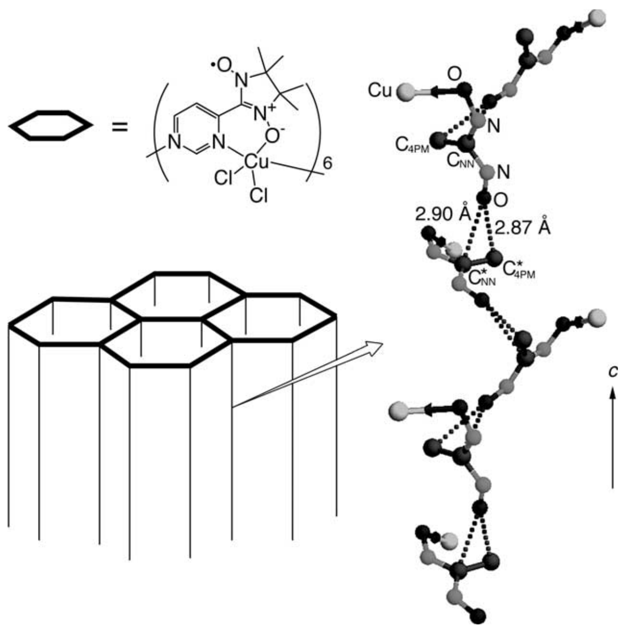

Fig. 4. (Left) Schematic drawing of the tube-like cavity in the crystal of **1**. (Right) Linear array of nitronyl nitroxide groups with a T-shaped configuration along the c-axis. Six ONC(–C)NO–Cu moieties are drawn. Interatomic distances within the sum of the van der Waals radii are shown with dotted lines. Symmetry operation code for * is $-y+2/3$, $x-y+1/3$, $z+1/3$.

We briefly review the magnetic coupling mechanisms in the crystal of **1** [3,4] in order to discuss the origin of the enhancement of ferromagnetic interaction. We can find a chelate structure in the repeating unit $CuCl_2 \cdot$(4PMNN), in which the nitronyl notroxide (NN) oxygen atom is axially coordinated to the copper ion. The orthogonality of Cu 3d$_{x^2-y^2}$ and O 2p$_z$ orbitals favors ferromagnetic interaction between the Cu and NN spins [5]. We can also find that the PM bridges two copper ions. We have clarified the relationship between coordination structures and magnetic couplings in PM-bridged copper(II) complexes [6–9]. In the present case, every PM nitrogen atom is coordinated at an equatorial position and consequently the PM bridge should be an antiferromagnetic coupler. Furthermore, relatively short van der Waals contacts between columns can be pointed out, as shown with dotted lines in Fig. 4. The shortest distance is found between a terminal NN oxygen atom and a carbon atom of the PM 4-position in a neighboring molecule ($O\cdots C_{4PM}$). The second shortest distance is found between a terminal NN oxygen atom and a central NN carbon atom ($O\cdots C_{NN}$). Almost vertical spatial arrangement of two NN units gives a T-shaped configuration. This contact brings about ferromagnetic coupling on the basis of McConnell's theory [10–12]. The geometry depicted in Fig. 4 infinitely repeats by a 3_1 screw symmetry along the c axis, i.e., perpendicular to the macrocyclic molecular plane, among the columns. Detailed analysis suggests that intermolecular ferromagnetic interaction competes with intramolecular antiferromagnetic interaction and that the increasing behavior of the $\chi_{\mathrm{mol}}T$ values on cooling from 100 to 7 K can be ascribed to the intermolecular interaction between the local $S=1$ units of the strongly correlated Cu and NN spins [3].

Now we will discuss what structural deformation affects the ferromagnetic coupling. We found a few correlations between the magnetic properties and cell parameters, as shown in Fig. 5(a) and (b). The cell volume (V) varied from 8561 to 8467 Å^3 and the $\chi_{\mathrm{mol}}T$ maximum varied from 4 to 17 cm^3 K mol^{-1}. Obviously the sample with a smaller cell volume shows stronger ferromagnetic interaction. Fig. 5(a) shows the $\chi_{\mathrm{mol}}T$ maximum vs. V plot for the complexes in the present study and also summarize the $\chi_{\mathrm{mol}}T$ maximum values for the complexes containing organic guest molecules which have been previously reported [4]. In order to elucidate which axis is responsible for the variation of the cell volume, we plotted the $\chi_{\mathrm{mol}}T$ maximum values against the a ($=b$) and c axes, and found a correlation

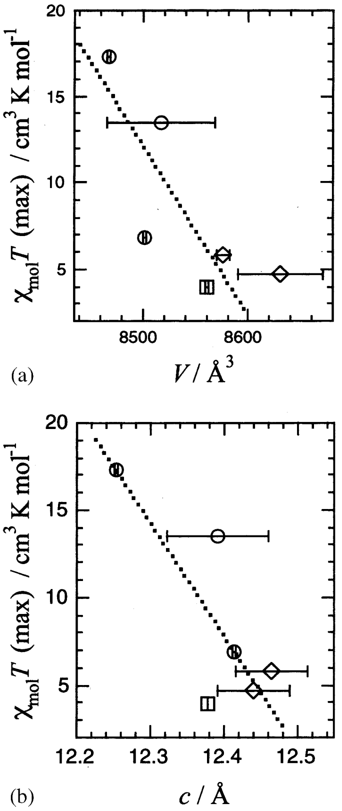

Fig. 5. Correlations between the $\chi_{\mathrm{mol}}T$ maximum value and the cell volume (V) (a) and between the $\chi_{\mathrm{mol}}T$ maximum value and the c length (b) for the host–guest compounds of **1**. Guest molecules are MCl (M = Li, Na, K) (circles), organic compounds [4] (diamonds), and none (squares). Dotted lines are shown for a guide to the eye.

with the *c* axis (Fig. 5(b)). The sample with a shorter *c* axis exhibits stronger ferromagnetic interaction, whilst the *a* axis is insensitive to the guest inclusion. This finding is rationalized by the fact that the rigid macrocyclic structure parallel to the *ab* plane is composed of covalent bonds. On the other hand, the column direction along the *c* axis can accommodate the cell shrinkage due to the guest inclusion, because the molecular stack was dominantly made with van der Waals interaction.

The guest inclusion causes to shrink the cell but not each molecule. The enhancement of the ferromagnetic interaction after the guest inclusion supports that the ferromagnetic interaction originates in the van der Waals contacts as depicted in Fig. 4. Therefore, we believe that shorter O···C distances in the T-shape arrangement of the radical moieties cause stronger ferromagnetic interaction. The shrinkage of the cell suggests the presence of attractive interaction in the host–guest system; in particular, the shortening of the *c* length may be interpreted in terms of guest–guest attractive interaction. There seem to be Coulombic interaction and hydrogen-bond interaction in $(\mathrm{MCl})_n$@**1** and $(\mathrm{H_2O})_n$@**1**, respectively, in the tube-like cavity along the *c* axis.

The guest inclusion accompanys not only shortening intermolecular contacts but also other possible geometrical deformation and electronic structural modification of the host, especially distortion of the magnetic orbital of the copper ion. Several factors are responsible for the variation of the magnetic behavior, and accordingly more detailed structural evidence could improve the understanding of the magneto-structure relationship.

5. Summary

Discrete hexanuclear complexes **1** and **2** construct a perfect column perpendicular to the macrocyclic molecular plane. The nano-scaled honeycomb-like channels are available for the host–guest complexes, and actually the magnetic properties are tuned by the inclusion. The present work can be regarded as an example of porous organic–inorganic hybrid solids utilized for chemically switchable magnetic materials.

Acknowledgements

This work was supported by a Grant-in-Aid for Scientific Research on Priority Areas of 'Molecular Conductors and Magnets' (No. 730/11224204) and by a Grant-in-Aid for Scientific Research (No. 13640575), both from the Ministry of Education, Culture, Sports, Science and Technology, Japan.

References

[1] (a) J.R. Friedman, M.P. Sarachik, J. Tejada, R. Ziolo, Phys. Rev. Lett. 76 (1996) 3830;
(b) L. Thomas, F. Lionti, R. Ballow, D. Gatteschi, R. Sessoli, B. Barbara, Nature 383 (1996) 145;
(c) W. Wernsdorfer, N. Allega-Alcalde, D.N. Hendrickson, G. Christou, Nature 416 (2002) 406.

[2] (a) Kusaka, T. Ishida, T. Nogami, Mol. Cryst. Liq. Cryst. 379 (2002) 259;
(b) K. Awaga, E. Coronado, M. Drillon, MRS Bull. (2000) 52;
(c) A. Rujiwatra, C.J. Kepert, J.B. Claridge, M.J. Rosseinsky, H. Kumagai, M. Kurmoo, J. Am. Chem. Soc. 123 (2001) 10584;
(d) S. Decurtins, R. Pellaux, G. Antorrena, F. Palacio, Coord. Chem. Rev. 190–192 (1999) 841;
(e) A. Cornia, M. Affronte, A.G.M. Jansen, G.L. Abbati, D. Gatteschi, Angew. Chem., Int. Ed. Engl. 38 (1999) 2264;
(f) A. Cornia, A. Caneschi, P. Dapporto, A.C. Fabretti, D. Gatteschi, W. Malavasi, C. Sangregorio, R. Sessoli, Angew. Chem., Int. Ed. Eng. 38 (1999) 1780;
(g) M. Nakano, A. Nakahama, S. Okuno, G.-E. Matsubayashi, W. Mori, M. Katada, Mol. Cryst. Liq. Cryst. 376 (2002) 399;
(h) C. Rancurel, N. Daro, O.B. Borobia, E. Herdtweck, J.-P. Sutter, Eur. J. Org. Chem. (2003) 167.

[3] J. Omata, T. Ishida, D. Hashizume, F. Iwasaki, T. Nogami, Inorg. Chem. 40 (2001) 3954.
[4] J. Omata, T. Ishida, D. Hashizume, F. Iwasaki, T. Nogami, Polyhedron 20 (2001) 1557.
[5] (a) A. Caneschi, D. Gatteschi, J. Laugier, P. Rey, J. Am. Chem. Soc. 109 (1987) 2191;
(b) A. Caneschi, D. Gatteschi, P. Rey, R. Sessoli, Acc. Chem. Res. 22 (1989) 392.
[6] T. Ishida, T. Kawakami, S.-I. Mitsubori, T. Nogami, K. Yamaguchi, H. Iwamura, J. Chem. Soc., Dalton Trans. (2002) 3177.
[7] (a) M. Yasui, Y. Ishikawa, N. Akiyama, T. Ishida, T. Nogami, F. Iwasaki, Acta Crystallogr., Sect. B 57 (2001) 288;
(b) F. Mohri, K. Yoshizawa, T. Yamabe, T. Ishida, T. Nogami, Mol. Eng. 8 (1999) 357;
(c) R. Feyerherm, S. Abens, D. Günther, T. Ishida, M. Meissner, M. Meschke, T. Nogami, M. Steiner, J. Phys.: Condens. Mat. 12 (2000) 8495.
[8] (a) T. Ishida, T. Nogami, Recent Res. Dev. Pure Appl. Chem. 1 (1997) 1;
(b) T. Ishida, K. Nakayama, M. Nakagawa, W. Sato, Y. Ishikawa, M. Yasui, F. Iwasaki, T. Nogami, Synthetic Met. 85 (1997) 1655.
[9] T. Ezuhara, K. Endo, K. Matsuda, Y. Aoyama, New J. Chem. 24 (2000) 609.
[10] H.M. McConnell, J. Chem. Phys. 39 (1963) 1910.
[11] (a) K. Inoue, H. Iwamura, Chem. Phys. Lett. 207 (1995) 551;
(b) T. Kawakami, A. Oda, W. Mori, K. Yamaguchi, K. Inoue, H. Iwamura, Mol. Cryst. Liq. Cryst. 279 (1996) 29.
[12] T. Kawakami, Y. Kitagawa, F. Matsuoka, Y. Yamashita, K. Yamaguchi, Polyhedron 20 (2001) 1235.